ELSEVIER

Nuclear Physics A 624 (1997) 257–274

NUCLEAR PHYSICS A

Collective γ-vibrational bands in ^{165}Ho and ^{167}Er

G. Gervais [a], D.C Radford [b], Y.R Shimizu [c], M Cromaz [d], J DeGraaf [d], T.E Drake [d], S. Flibotte [a,b], A Galindo-Uribarri [b], D.S Haslip [a], V.P Janzen [b], M Matsuzaki [e], S.M. Mullins [a,1], J.M Nieminen [a], C.E Svensson [a], J.C Waddington [a], D Ward [b], J.N. Wilson [a]

[a] *Department of Physics and Astronomy, McMaster University, Hamilton, ON L8S 4M1, Canada*
[b] *AECL, Chalk River Laboratories, Chalk River, ON K0J 1J0, Canada*
[c] *Department of Physics, Kyushu University, Fukuoka 812, Japan*
[d] *Department of Physics, University of Toronto, Toronto, ON M5S 1A7, Canada*
[e] *Department of Physics, Fukuoka University of Education, Munakata, Fukuoka 811-41, Japan*

Received 4 February 1997; revised 27 March 1997

Abstract

The nuclear structures of ^{165}Ho and ^{167}Er have been investigated by means of Coulomb excitation. These nuclei excited at moderate spins exhibit γ-vibrational bands with $K^\pi = \frac{11}{2}^-, \frac{3}{2}^-$ in ^{165}Ho and $K^\pi = \frac{11}{2}^+$ in ^{167}Er. The γ-vibrational bands in ^{165}Ho are found to be isospectral; having very nearly identical in-band γ-ray energies. Gamma-ray branching ratios are analysed to extract information on collectivity and Coriolis mixing. Experimental results are compared with calculations performed with the Cranked Shell Model + RPA + particle–vibration coupling and by invoking the generalized intensity relations (GIR) in the unified model scheme. Although this model explains many features of the data, puzzling aspects such as identical transition energies for the bands in ^{165}Ho remain unexplained. The role of the K quantum number in identical bands is discussed. © 1997 Elsevier Science B.V.

Keywords: Coulomb excitation, ^{165}Ho, ^{167}Er, thick gold-backed target; ^{209}Bi beam $E = 5.4$ MeV/u; Measured E_γ, I_γ, γ–γ coincidences; Deduced level schemes, $K = \frac{3}{2}, \frac{11}{2}$; γ-vibrational bands; Compton-suppressed HPGe detector array, 4π-BGO ball; Cranked Shell Model + RPA + particle–vibration coupling calculations; Generalized intensity relations; Experimental Routhians; Calculated and deduced signature splitting energies, intrinsic moment ratios; Identical bands

[1] Present address: Department of Nuclear Physics, ANU, Canberra, ACT 0200, Australia.

PII S0375-9474(96)00320-5

1. Introduction

The recent discovery of identical superdeformed bands in neighbouring nuclei [1] has lead to numerous theoretical and experimental investigations. Many models have been proposed to explain the origin of this phenomenon but a complete understanding of these bands is still elusive. A recent review article of the subject can be found in Ref. [2]. A simpler case of identical bands, such as isospectral bands in the same nucleus, would perhaps assist in obtaining a deeper theoretical understanding of the more complex cases. A possible candidate for such a set of bands is a pair of collective γ-vibrational bands built on the ground-state configuration of an odd-mass nucleus. Although the quasiparticle excitations in rapidly rotating nuclei have been well studied, collective vibrational bands have not been well investigated experimentally, particularly in odd-mass nuclei.

Rare-earth nuclei, such as ^{165}Ho and ^{167}Er, have large quadrupole deformation in their ground states ($\epsilon_2 = 0.274$ for both nuclei) and exhibit both rotational and vibrational motions. High-spin states in these neutron-rich stable nuclei can not be reached in fusion-evaporation reactions but they can be populated by Coulomb excitation. Both nuclei have been studied previously by this technique and vibrational bands were observed to low spins [3–6]. The present article reports on experiments designed to extend the vibrational bands to higher spins.

Electromagnetic transition properties such as the $B(\mathcal{M}\lambda)$ values can be extracted from the experimental branching ratios of either in-band or out-of-band transitions. They provide important information on the collectivity and Coriolis mixing and can readily be compared with theoretical predictions. Theoretical calculations are usually based on the Cranked Shell Model at the high-spin limit [7]. However, at relatively low-spin, the effects of the angular momentum algebra become important. To take this effect into account, a new method combining the generalized intensity relations (GIR) [8] and the Cranked Shell Model has been developed [9]. The calculated transition quadrupole moments for the γ-vibrational bands in this new theoretical approach will be compared with the experimental values. The role of the K quantum number in identical bands will also be discussed.

2. Experimental details

Excited states in ^{165}Ho and ^{167}Er nuclei have been populated by Coulomb excitation with a ^{209}Bi beam of 5.4 MeV per nucleon provided by the TASCC facility at the Chalk River Laboratories. With its large atomic number, the ^{209}Bi nucleus is very effective in Coulomb exciting the target to high angular momenta. The beam energy was chosen to be above the "safe energy" [10] ($\sim 4.5A$ MeV) in order to maximize the population of high-spin states. Therefore, the excitation process was not purely electromagnetic since, considering the deformation of the target nuclei, the distance of closest approach for some trajectories could be within the range of the nuclear interaction. It should be

noted that this choice of beam energy does not allow us to extract the *absolute* electromagnetic transition probabilities through an analysis of the cross-section based on the Coulomb excitation process (e.g. Ref. [10]). The γ-rays emitted in the decay of excited states were detected with the 8π Spectrometer [11], an array which comprises a bismuth germanate (BGO) ball of 71 elements and 20 Compton-suppressed hyperpure germanium (HPGe) detectors. The HPGe detectors were calibrated for efficiency with standard radioactive sources (^{152}Eu and ^{133}Ba). Two separate experiments were performed for ^{165}Ho. In the first one, a thick ^{165}Ho target was used, and 1.6×10^6 γ–γ events were collected in the HPGe array with a condition that at least 3 elements of the BGO ball fired in time coincidence ($K_{\mathrm{BGO}} \geqslant 3$). For the second experiment, the target consisted of 2 mg/cm^2 of ^{165}Ho on a thick gold backing (43.8 mg/cm^2) which stopped the recoiling nuclei more quickly than in holmium material. In experiments with Au as a target, we have noted that the cross-sections are much smaller than in either ^{165}Ho or ^{167}Er and gold was considered as the best possible backing. Over 2×10^6 γ–γ events were collected in this experiment, with the same fold requirement ($K_{\mathrm{BGO}} \geqslant 3$) in the BGO ball. The experiment for ^{167}Er was performed with a target consisting of a foil of ^{167}Er (1.87 mg/cm^2) with a gold backing (43.8 mg/cm^2). A total of 4×10^6 γ–γ events were collected with the condition $K_{\mathrm{BGO}} \geqslant 3$.

3. Data analysis and level schemes

The E_γ–E_γ coincidence events recorded in the HPGe array were sorted into γ–γ matrices. No extra conditions were set on the number of BGO elements that fired. Figs. 1 and 2 show the total projection of the resulting symmetrized matrices for ^{165}Ho and ^{167}Er, respectively. The peak-to-background ratio is approximatively 13 : 1 for the 257 keV $\frac{15}{2}^+ \rightarrow \frac{11}{2}^+$ transition in the ground-state band of ^{167}Er. This ratio is characteristic of Coulomb excitation. If the nucleus is excited to a region of low level density, a smaller amount of continuum is observed as compared to a fusion-evaporation process in which the nucleus decays from a region of high level density. The level schemes were built with the help of the computer codes GF2 and ESCL8R [12]. Figs. 3 and 4 show the proposed level schemes for both nuclei. Six rotational bands were observed in ^{165}Ho and five were observed in ^{167}Er. The bandhead spins are those previously assigned [3–6,13].

In the ^{165}Ho nucleus, the ground-state band is built on the single-particle configuration $\frac{7}{2}^-[523]$ which arises from the $h_{\frac{11}{2}}$ proton orbital. It was extended to spin $\frac{39}{2}$ and two γ-vibrational bands were also populated. These vibrational bands have $K^\pi = \frac{11}{2}^-$ and $K^\pi = \frac{3}{2}^-$, resulting from the parallel and anti-parallel alignment of the $K = 2$ γ phonon with the $K_{\mathrm{gr}} = \frac{7}{2}$ unpaired proton. These two rotational bands were extended from spins $\frac{15}{2}$ and $\frac{13}{2}$ to $\frac{37}{2}$ and $\frac{33}{2}$, respectively. Gamma-ray spectra corresponding to these bands are shown in Fig. 1. The rotational bands built on the proton configuration $\frac{3}{2}^+[411]$ and $\frac{1}{2}^+[411]$ were also observed at higher spins. Two new structures (labeled A) were

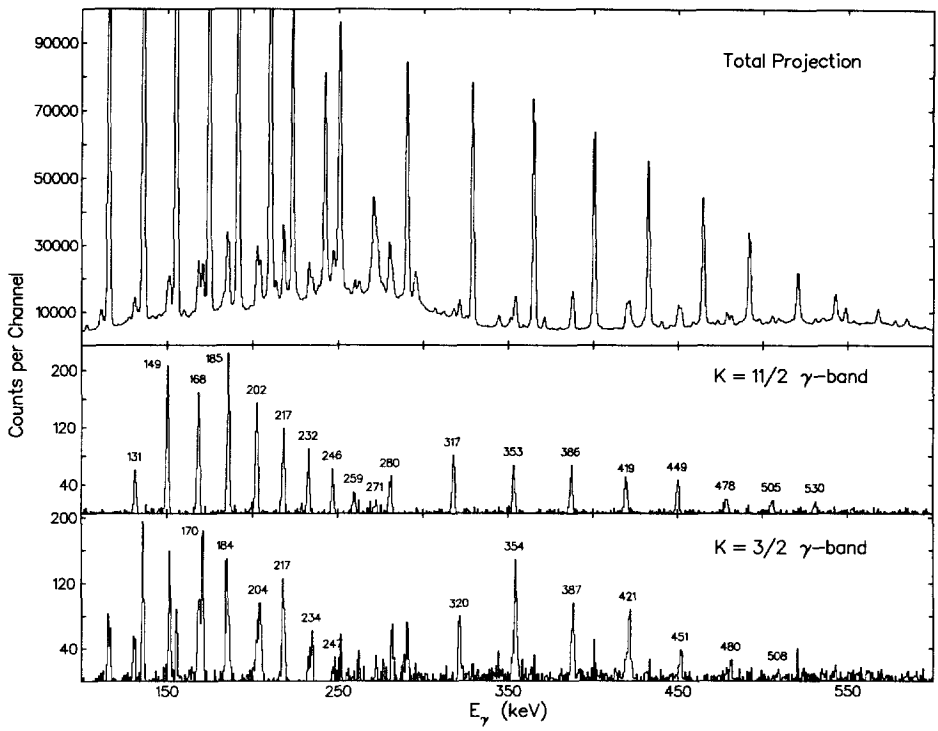

Fig. 1. Spectra gated on transitions from $K = \frac{3}{2}$ and $K = \frac{11}{2}$ γ-vibrational bands in ^{165}Ho, together with the total projection spectrum. These spectra were taken from the experiment performed with the gold-backed target.

also observed and are shown in Fig. 3. They appear to form a coupled band with large signature splitting; it has not been possible to assign these rotational bands to any known bandhead. The spins of the energy levels for these two bands were assigned by studying the decay-out to known structures. However, the spin assignments are tentative and it is impossible to draw any conclusion concerning the exact nature of these two new structures. An indication of the observed population intensity of each band in ^{165}Ho is given in Table 1.

The ground-state band in ^{167}Er is built on the configuration $\frac{7}{2}^+[633]$, arising from the $i_{\frac{13}{2}}$ neutron intruder orbital. This band has been extended from spin $\frac{25}{2}$ to spin $\frac{37}{2}$. Two single-neutron excitations, $\frac{1}{2}^-[521]$ and $\frac{5}{2}^-[512]$, have been Coulomb excited for the first time and were observed to spins $\frac{37}{2}$ and $\frac{27}{2}$, respectively. The $K^\pi = \frac{11}{2}^+$ γ-vibrational band was extended from $\frac{17}{2}$ to $\frac{37}{2}$. This collective excitation results from the parallel alignment of the $K = 2$ γ phonon with the $K_{gr} = \frac{7}{2}$ unpaired neutron. Two other structures (labeled B) have been observed, forming a coupled band, but were not assigned to any known bandhead. The most likely spins of this band were determined by studying the decay-out to the ground-state band. This band could be the missing anti-parallel alignment $K^\pi = \frac{3}{2}^+$ γ-vibration band. However, an attempt to extrapolate the

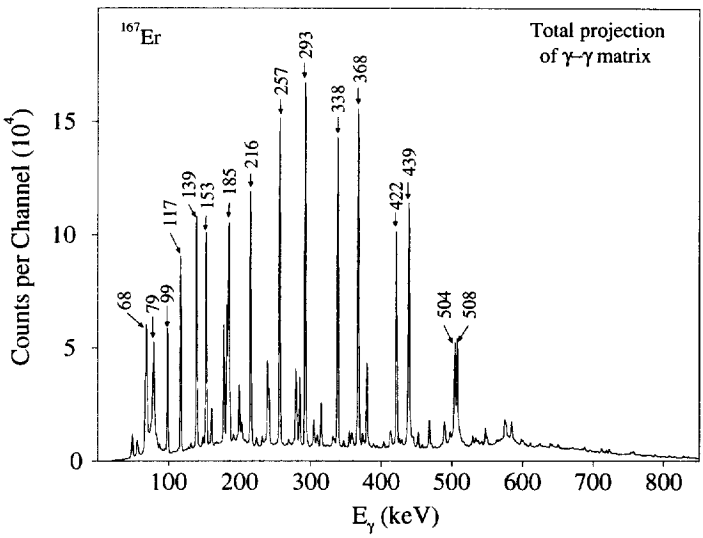

Fig. 2. Total projection of the symmetrized γ–γ coincidence matrix for ^{167}Er. The strongest γ-rays are labeled by their energies in keV.

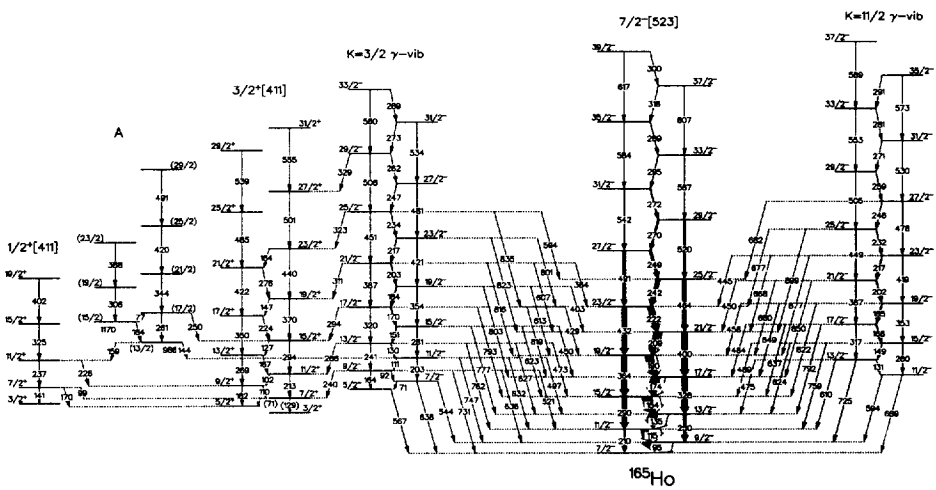

Fig. 3. Proposed level scheme for ^{165}Ho. The width of the arrows is proportional to the transition intensity and an open space represents the intensity carried by internal conversion. The assignments are labeled with the Nilsson number $K\pi[Nn_z\Lambda]$ for the ground-state band and for the single-proton excitations and by K for the vibrational bands. The spins within parentheses indicate tentative assignments.

experimental Routhians [14] with the known levels of $K^\pi = \frac{3}{2}^+$ γ-vibration band was inconclusive. Typical spectra of the bands are shown in Figs. 5 and 6 and an indication of the observed population intensity of each band in ^{167}Er is given in Table 2.

In these experiments, the recoiling nuclei were not detected and the γ-ray energies

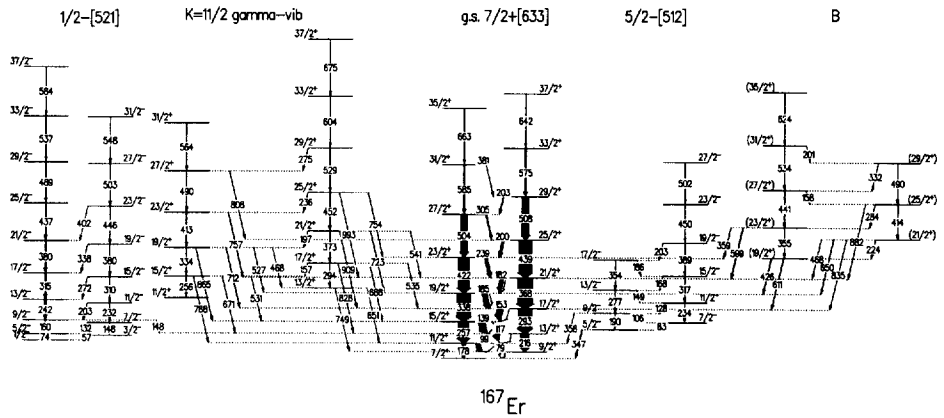

Fig. 4. Proposed level scheme for ^{167}Er. The width of the arrows is proportional to the transition intensity and an open space represents the intensity carried by internal conversion. The assignments are labeled with the Nilsson number $K\pi[Nn_z\Lambda]$ for the ground-state band and for the single-neutron excitations and by K for the γ vibration. The spins within parentheses indicate tentative assignments.

Table 1
Relative intensities of the bands observed in ^{165}Ho. The relative intensity was defined as: (Intensity of most intense stretched E2 γ-ray in the band) / (Intensity of most intense stretched E2 γ-ray in the g.s. band)

Band	Signature α	Most intense γ-ray [keV]	Relative intensity [%]
$\frac{7}{2}^-$[523] g.s.	$-\frac{1}{2}$	364	≡100
$\frac{7}{2}^-$[523] g.s.	$\frac{1}{2}$	400	94(6)
$\frac{11}{2}^-$ γ-vib.	$-\frac{1}{2}$	419	8.3(7)
$\frac{11}{2}^-$ γ-vib.	$\frac{1}{2}$	387	9.8(7)
$\frac{3}{2}^-$ γ-vib.	$-\frac{1}{2}$	354	8.5(6)
$\frac{3}{2}^-$ γ-vib.	$\frac{1}{2}$	386	8.5(6)
$\frac{3}{2}^+$[411]	$-\frac{1}{2}$	294	4.4(4)
$\frac{3}{2}^+$[411]	$\frac{1}{2}$	269	3.9(4)
$\frac{1}{2}^+$[411]	$-\frac{1}{2}$	237	1.8(2)
unassigned	$-\frac{1}{2}$	419	0.62(8)
unassigned	$\frac{1}{2}$	306	2.1(2)

were not corrected for Doppler shift. Therefore, the maximum spin observed depends strongly on the stopping time of the nuclei. For ^{165}Ho, the faster stopping time in the gold-backed target, compared with the thick ^{165}Ho target, allowed the observation of typically one or two more transitions at the top of each band. However, the γ-rays associated with the population of the highest-spin states were emitted from a moving nucleus and were thus Doppler broadened. The γ-ray peaks corresponding to the highest transitions observed possessed only a small "stopped" component. Typical examples are

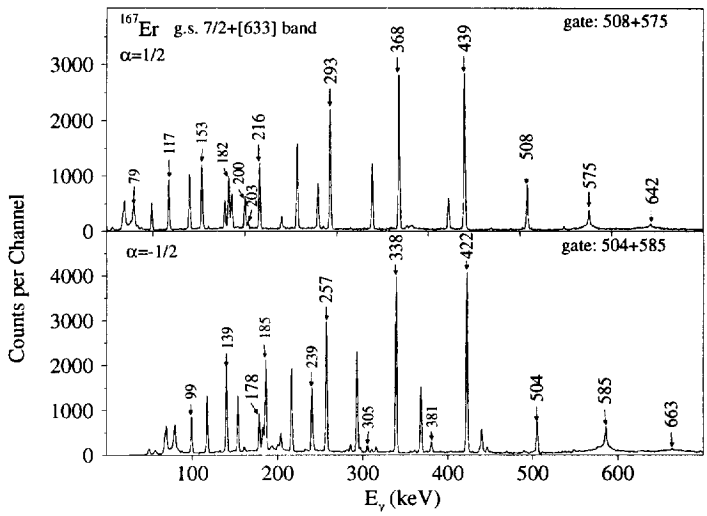

Fig. 5. Coincidence γ-ray spectra for the ground-state band in ^{167}Er. Each spectrum is labeled by the signature $\alpha = \pm\frac{1}{2}$ and the γ-ray energies are given in keV. Each spectrum corresponds to a sum of two gates, set on the 508+575 keV peaks for $\alpha = \frac{1}{2}$ and on the 504+585 keV peaks for $\alpha = -\frac{1}{2}$, respectively.

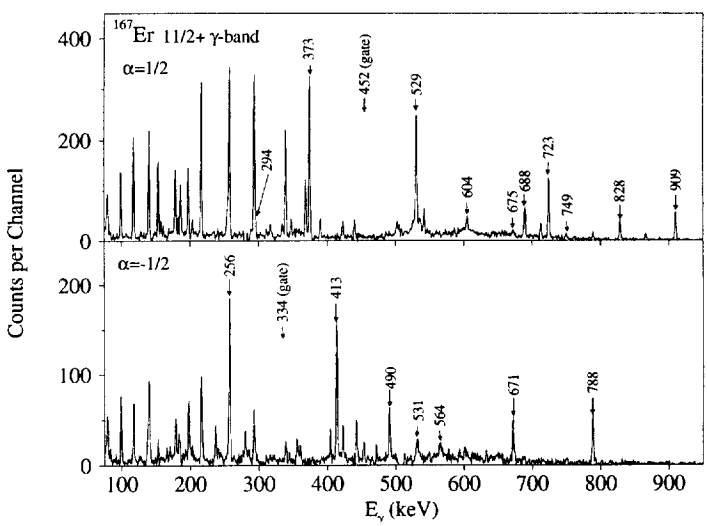

Fig. 6. Coincidence γ-ray spectra for the $K = \frac{11}{2}$ γ-vibration band in ^{167}Er. Each spectrum is labeled by the signature $\alpha = \pm\frac{1}{2}$ and the γ-ray energies of the band are given in keV. The spectra were obtained with a gate set on the 452 keV γ-ray for $\alpha = \frac{1}{2}$ and on the 334 keV γ-ray for $\alpha = -\frac{1}{2}$. For $\alpha = \frac{1}{2}$, the 294 keV γ ray is on the right side of the strong 293 keV peak from the ground-state band.

the 575 and 585 keV γ-rays in the ground-state band of ^{167}Er (cf. Fig. 5) which exhibit a characteristic Doppler broadening. Setting an energy window on the stopped component of a peak selects the events where the nucleus has decayed at rest, which increases the resolving power for states at higher spins. However, the number of events

Table 2
Relative intensities of the bands observed in ^{167}Er. The relative intensity was defined as in Table 1

Band	Signature α	Most intense γ-ray [keV]	Relative intensity [%]
$\frac{7}{2}^+[633]$ g.s.	$\frac{1}{2}$	368	≡100
$\frac{7}{2}^+[633]$ g.s.	$-\frac{1}{2}$	338	87(4)
$\frac{11}{2}^+\gamma$-vib.	$\frac{1}{2}$	452	6.1(3)
$\frac{11}{2}^+\gamma$-vib.	$-\frac{1}{2}$	413	4.6(3)
$\frac{1}{2}^-[521]$	$\frac{1}{2}$	242	9.4(5)
$\frac{1}{2}^-[521]$	$-\frac{1}{2}$	380	2.4(1)
$\frac{5}{2}^-[512]$	$\frac{1}{2}$	354	0.64(6)
$\frac{5}{2}^-[512]$	$-\frac{1}{2}$	389	0.59(5)
unassigned	$\frac{1}{2}$	414	3.2(2)
unassigned	$-\frac{1}{2}$	441	6.8(3)

Table 3
Relative γ-ray intensity as a function of spin for stopped nuclei for the $\alpha = \frac{1}{2}$ signature of the ground-state band in ^{167}Er. The relative intensity was defined as: (Intensity of most intense γ-ray in the gate)/(Most intense γ-γ coincidence in the whole matrix)

Gate	Spin J_i	Most intense γ-ray [keV]	Relative intensity [%]
216	$\frac{13}{2}$	293	38(1)
293	$\frac{17}{2}$	368	86(2)
368	$\frac{21}{2}$	439	≡100
439	$\frac{25}{2}$	368	≡100
508	$\frac{29}{2}$	439	53(2)
575	$\frac{33}{2}$	508	16(1)
642	$\frac{37}{2}$	575	1.3(2)

associated with stopped nuclei drops drastically at high spins, which is a limitation of the technique used. Table 3 gives the typical relative intensity of γ-rays within the signature $\alpha = \frac{1}{2}$ of the ground-state band in ^{167}Er. For each $J \rightarrow J-2$ in-band transition, the number of counts in the coincidence spectrum generated by an energy window set on the stopped component of the γ-ray peak decreases as the spin of the gating transition increases. For the highest spins observed, only a few events have occurred when the nucleus was at rest. It is possible that the nucleus was Coulomb excited to higher angular momenta but, in these cases, the stopped component of the peaks has vanished. A previous Coulomb excitation performed on ^{238}U with the 8π Spectrometer reached up to $31\hbar$ [14]. Although the recoil was stopped more slowly by the ^{238}U thick target, higher spin transitions were observable because the lifetimes of a given spin are much longer in ^{238}U.

4. Theory and details of calculations

The calculations were performed with the Cranked Shell Model. The vibrational excitations were treated within the formalism of the random phase approximation (RPA) [15,16]. This microscopic mean-field approach takes into account the effects of deformation, pairing correlations and rotational motion on the quasiparticle energies. For odd-mass nuclei, effects of coupling between the unpaired quasiparticle and the vibrational modes should be taken into account in order to describe correctly the electromagnetic transition properties of the vibrational bands. In Ref. [17], such an approach is developed and successfully applied to investigate the polarization effect of the vibrational motions on the electromagnetic properties of various one-quasiparticle rotational bands at high spins. In the present study, the experimental data give direct information about the vibrational motion in rotating odd-mass nuclei. In this respect, the interband E2 transitions from the γ-vibrational bands to the ground-state band are especially interesting in the study of collectivity. The intraband $\Delta J = 1$ E2 and M1 transitions can give other information, such as the triaxiality of the mean field.

It should be emphasized that the method to calculate the electromagnetic transition probabilities in Ref. [17] is based on the semi-classical cranking model in the high-spin limit [7]. However, for relatively low-spin transitions, the quantum mechanical effects of the angular momentum algebra (i.e. the Clebsch–Gordan coefficients) are important and should be fully taken into account. A new method has been developed recently [9] (see also Ref. [18]) to overcome this difficulty by invoking the generalized intensity relations (GIR) in the unified model [8], where the angular momentum algebra is treated in a full quantum mechanical approach. According to this method, the intrinsic parameters appearing in the GIR are uniquely related to the matrix elements evaluated at the zero-frequency limit in the cranking model. Therefore, the microscopic approaches mentioned above [16,17] can be straightforwardly applied.

For the γ bands, the intrinsic moments of the out-of-band and in-band E2 transitions are extracted from the equations

$$\left[B(\mathrm{E2}: J_\mathrm{i}^{(\gamma)} \to J_\mathrm{f}^{(\mathrm{g.s.})}\right]^{1/2} = \langle J_\mathrm{i} K_\mathrm{i} 2 \Delta K | J_\mathrm{f} K_\mathrm{f}\rangle \, Q_\mathrm{out},$$
$$\left[B(\mathrm{E2}: J_\mathrm{i}^{(\gamma)} \to J_\mathrm{i}^{(\gamma)} - 2)\right]^{1/2} = \langle J_\mathrm{i} K_\mathrm{i} 20 | J_\mathrm{i} - 2K_\mathrm{i}\rangle \, Q_\mathrm{in}. \qquad (1)$$

Up to the first order in the GIR, the spin dependence of the intrinsic moments Q_in and Q_out can be written as [2]

$$Q_\mathrm{in} = Q_0, \qquad Q_\mathrm{out} = Q_1 + Q_2 \left[J_\mathrm{f}(J_\mathrm{f}+1) - J_\mathrm{i}(J_\mathrm{i}+1)\right], \qquad (2)$$

[2] More precisely, Q_in has a first order correction term for $K \neq 0$ bands. However, it is typically two or three orders of magnitude smaller than Q_0 for in-band stretched E2 transitions in well-deformed nuclei and can therefore be neglected [9].

Table 4
Basic parameters used in the calculations. A reduction factor of 0.8 was introduced in the pairing gap of the unpaired nucleon to account for the blocking effect. All the parameters are independent of the rotational frequency ω_{rot} and were not adjusted to reproduce the experimental results obtained in the present work

	ϵ_2	Δ_n (MeV)	Δ_p (MeV)	$\hbar\omega_\beta$ (MeV)	$\hbar\omega_\gamma$ (MeV)	$\hbar\omega_{NG}$ (MeV)	$\mathcal{J}$ ($\hbar^2$/MeV)
^{167}Er	0.274	0.871×0.8	0.868	1.339	0.804	0	55.9
^{165}Ho	0.274	0.899	0.841×0.8	1.460	0.774	0	47.8

where $Q_{0,1,2}$ are constants within the first order approximation. The absolute value of E2 transition probabilities were not measured in the present work. However, the ratio of transition amplitudes parametrized by

$$\frac{Q_{out}}{Q_{in}} = \frac{Q_1}{Q_0} + \frac{Q_2}{Q_0}\left[J_f(J_f+1) - J_i(J_i+1)\right], \tag{3}$$

can be deduced from the experimental branching ratio.

According to Ref. [9], the intrinsic parameters in Eq. (2) are calculated as follows:

$$\begin{aligned} Q_0 &= \left[\langle i|Q_{20}^{(+)}|i\rangle\right]_0, \\ Q_1 &= \sqrt{2}\,Q_{tr} - \Delta K(K_i + K_f)\,Q_2, \qquad Q_{tr} = \left[\langle f|Q_{22}^{(+)}|i\rangle\right]_0, \\ Q_2 &= \frac{1}{\sqrt{2}\,\mathcal{J}}\left[\frac{d\langle f|Q_{21}^{(+)}|i\rangle}{d\omega_{rot}}\right]_0, \end{aligned} \tag{4}$$

where $|i\rangle$ ($|f\rangle$) is the initial (final) state calculated by the microscopic cranking model, $Q_{2K}^{(+)}$ ($K = 0, 1, 2$) is the signature-coupled electric quadrupole operator, $\mathcal{J}$ is the moment of inertia of the band, and $[*]_0$ denotes that the quantities are evaluated at $\omega_{rot} \to 0$.

The details of the calculations are the same as in Ref. [18]. The quasiparticles and vibrational modes are obtained by the cranked mean-field theory and the RPA, with the inclusion of the particle–vibration coupling in the rotating frame. All the parameters in the model are determined independently. Table 4 summarizes the parameters used in the calculations. The pairing force strengths are fixed to reproduce the even–odd mass differences for neutrons and protons at $\omega_{rot} = 0$. A reduction factor of 0.8 for the odd-particle pairing gap is introduced to account for the blocking effect. The (isoscalar) quadrupole interaction strengths for the $K = 0, 1, 2$ components are determined at $\omega_{rot} = 0$ to reproduce $\hbar\omega_\beta$, $\hbar\omega_{NG}$ and $\hbar\omega_\gamma$ respectively, where NG stands for the Nambu–Goldstone (symmetry restoring) mode. The energies of the β and γ vibrations are taken from the average of neighbouring nuclei (since no data were available for the β vibration in ^{164}Dy, $\hbar\omega_\beta$ was taken from ^{166}Er). It should be noted that the quasiparticle–vibration coupling strengths are automatically determined by the quadrupole interaction strengths. The moment of inertia appearing in Eq. (4) was taken from the ground-state

Table 5
Calculated properties of the γ-vibrational bands built on the ground-state band with $K_{gr} = \frac{7}{2}$. For each vibrational mode with $K_> = \frac{11}{2}$ and $K_< = \frac{3}{2}$, the relative Routhians at $\omega_{rot} = 0$, $E'_{rel}(0)$, and the ratios Q_1/Q_0 and Q_2/Q_0 are compared with the experimental values. The values of $\mathcal{J}$ used to calculate the relative Routhians can be found in Table IV. No data being available in the present work for the $K = \frac{3}{2}$ γ vibration in ^{167}Er, the experimental relative Routhian was calculated with the excitation energy previously reported [13]

	K		$E'_{rel}(0)$ (keV)	Q_1/Q_0	Q_2/Q_0	Q_0 (eb)	Q_{tr} (eb)	Q_1 (eb)	Q_2 (eb)
^{165}Ho	$\frac{11}{2}$	cal.	591	0.175	0.0025	2.267	0.208	0.397	0.0057
	$\frac{11}{2}$	exp.	668	0.143(4)	0.0022(2)	–	–	–	–
	$\frac{3}{2}$	cal.	546	0.110	0.0021	2.266	0.209	0.248	0.0048
	$\frac{3}{2}$	exp.	536	0.086(2)	0.0021(1)	–	–	–	–
^{167}Er	$\frac{11}{2}$	cal.	592	0.142	0.0014	2.299	0.190	0.327	0.0033
	$\frac{11}{2}$	exp.	693	0.143(3)	0.0020(1)	–	–	–	–
	$\frac{3}{2}$	cal.	531	0.103	0.0013	2.299	0.188	0.236	0.0030
	$\frac{3}{2}$	exp.	549	–	–	–	–	–	–

band near the bandhead. The results of the calculations for both ^{165}Ho and ^{167}Er are summarized in Table 5.

5. Results and discussion

One of the novel results of the experiments is that γ-vibrational bands built on the one-quasiparticle ground-state bands of ^{165}Ho and ^{167}Er have been extended to moderate spins and ratios of transition quadrupole moments have been deduced from the experimental branching ratios. The K quantum number of the vibrational states results from the coupling of the collective and single-particle degrees of freedom. Two coupling modes are allowed; both parallel ($K_> = \frac{11}{2}$) and anti-parallel ($K_< = \frac{3}{2}$) alignments. In ^{165}Ho, these two coupling modes are strongly populated but only the parallel coupling is observed for ^{167}Er in the present study. The electromagnetic decays of the γ bands to the ground-state band give an opportunity to study the collectivity and Coriolis mixing for both coupling modes.

Fig. 7 shows the experimental Routhians for the ground-state and γ-vibrational bands in ^{165}Ho and ^{167}Er. No significant signature splitting is observed in the γ-vibration bands of either nucleus. However, the ground-state bands of these two nuclei show signature dependence of the quasiparticles energies, especially in ^{167}Er where the $\frac{7}{2}^+[633]$ quasineutron arising from the $i_{\frac{13}{2}}$ orbital becomes strongly Coriolis mixed as ω_{rot} increases [19]. Calculated and observed signature splitting energies in ^{167}Er are shown in Fig. 8. The absence of signature splitting in the γ-vibrational bands is not well reproduced by the calculations. The calculations underestimate the signature splitting energies in the ground-state band and also predict an increase of the splitting for γ bands while it is experimentally non-existent. In the particle–vibration coupling scheme, the resultant

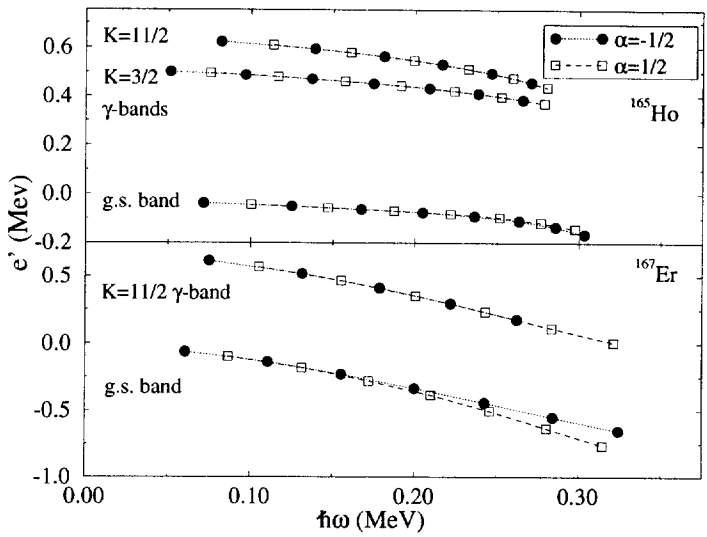

Fig. 7. Experimental Routhians for the ground-state and γ bands in ^{165}Ho (upper panel) and ^{167}Er (lower panel). References parametrized with the Harris parameters $\mathcal{J}_0 = 44.5$ MeV$^{-1}\hbar^2$ and $\mathcal{J}_1 = 110.0$ MeV$^{-3}\hbar^4$ for ^{165}Ho and $\mathcal{J}_0 = 37.2$ MeV$^{-1}\hbar^2$ and $\mathcal{J}_1 = 63.1$ MeV$^{-3}\hbar^4$ for ^{167}Er have been subtracted.

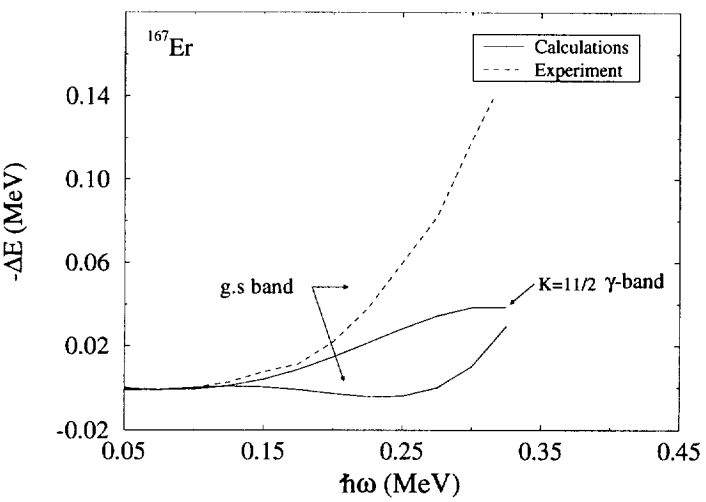

Fig. 8. Signature splitting in ^{167}Er defined by $\Delta E = E(\alpha = \frac{1}{2}) - E(\alpha = -\frac{1}{2})$ (MeV) as a function of the rotational frequency. For the $i_{\frac{13}{2}}$ orbital, ΔE is negative when the normal phase rule $\Delta E = (-1)^{j+\frac{1}{2}}|\Delta E|$ is assumed and so $-\Delta E$ was plotted. Experimentally, no significant signature splitting is observed in the γ-vibrational bands of either ^{167}Er or ^{165}Ho (not shown in the figure).

signature for a γ-vibrational band in an odd-mass nucleus depends on the signature of both the quasiparticle ($\alpha_{qp} = \pm\frac{1}{2}$) and the generalized γ-vibration mode ($\alpha_\gamma = 0, 1$) (see Ref. [17]). In this theoretical scheme, the signature splitting is affected by the coupling between collective and single-particle motions. The failure of the present calcu-

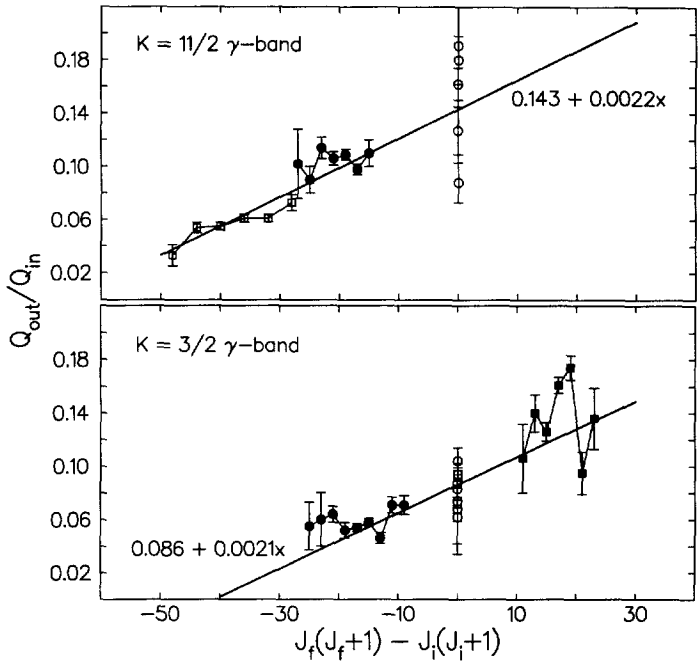

Fig. 9. Modified Mikhailov plot of the deduced ratios of transition quadrupole moments for the two γ bands in ^{165}Ho. The solid lines are least-squares fits to the experimental data where $x = J_f(J_f+1) - J_i(J_i+1)$.

lations to reproduce the experimental trend suggests that further theoretical investigations are needed in order to understand the exact origin of the absence of signature splitting for the quasiparticle + one-phonon states.

Experimental and calculated relative Routhians at $\omega_{rot} = 0$ are presented in Table 5. The experimental values of the relative Routhians at $\omega_{rot} = 0$ are obtained by $E'_{rel}(0) = E_{J=K} - \hbar^2(K - K_{gr})/(2\mathcal{J})$, where $E_{J=K}$ is the excitation energy of the bandhead, $\mathcal{J}$ and K_{gr} are the moment of inertia and the spin projection of the ground-state band, respectively. The moment of inertias of the γ-vibrational and ground state bands are assumed to be the same in the calculations of the relative Routhians, which is a good approximation in this case. The K-splitting of the relative Routhians at $\omega_{rot} = 0$ is underestimated by the calculations in both nuclei. The calculations of the $K = \frac{3}{2}$ γ band agree with the experimental values within 20 keV, while they underestimate the relative Routhians by $\sim$100 keV for the $K = \frac{11}{2}$ γ bands. Previous calculations of γ vibrations in odd-mass rare-earth nuclei [20] gave more or less the same trend.

Many transitions were observed from the decay-out of the γ bands. For ^{165}Ho and $K^\pi = \frac{3}{2}^-$, we observed $J \rightarrow J+1$, $J \rightarrow J$ and $J \rightarrow J-1$, while for $K^\pi = \frac{11}{2}^-$ we observed $J \rightarrow J$, $J \rightarrow J-1$ and $J \rightarrow J-2$. Several out-of-band transitions were also observed in ^{167}Er. If these transitions were between pure-K states, any M1 component with $|\Delta K| - \lambda = 1$ would be K-forbidden in the lowest order of the Coriolis coupling. Assuming that they are indeed pure E2, we can then use the experimental

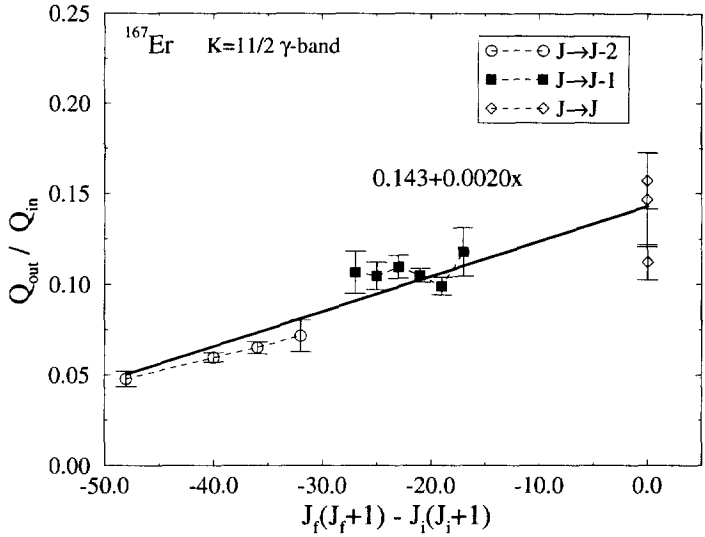

Fig. 10. Modified Mikhailov plot of the deduced ratios of transition quadrupole moments for the $K = \frac{11}{2}$ γ band in ^{167}Er. The solid line is the result of a least-squares fit to the experimental data where $x = J_f(J_f+1) - J_i(J_i+1)$.

branching ratios to calculate the ratio of intrinsic moments Q_{out}/Q_{in} which is related to the reduced matrix elements ($B(E2)$) by Eq. (1). Namely, Q_{out}/Q_{in} can be extracted from the branching ratio λ_{branch} by the relation:

$$\frac{Q_{out}}{Q_{in}} = \frac{\langle J_i K_i 20 | J_i - 2 K_i \rangle}{\langle J_i K_i 2 \Delta K | J_f K_f \rangle} \left[\frac{E_\gamma^{in}(J_i \to J_i - 2)}{E_\gamma^{out}(J_i \to J_f)} \right]^{5/2} \frac{1}{\sqrt{\lambda_{branch}}}. \tag{5}$$

We can therefore make a (modified) Mikhailov plot [21] of Q_{out}/Q_{in} versus $x = J_f(J_f+1) - J_i(J_i+1)$. In a Mikhailov plot, the slope provides a measurement of the spin-independent Coriolis-mixing amplitude ($\propto Q_2$) and the intercept gives a measurement of the direct intrinsic transition $\Delta K = 2$ matrix element ($\propto Q_1$). Our Mikhailov plot is modified by the necessity to introduce Q_{in} (coming from the branching ratio) and so the slope and intercept are related to the ratios Q_2/Q_0 and $Q_1 Q_0$, respectively. In Figs. 9 and 10, modified Mikhailov plots are presented for the γ bands observed in ^{165}Ho and ^{167}Er. The data from these figures are not inconsistent with a linear dependence on x. The parameters Q_1/Q_0 and Q_2/Q_0 from Eq. (3) were extracted from these figures and are presented in Table 5. The agreement with the calculations is good. In particular, the differences between the $K_>$ and $K_<$ coupling modes in ^{165}Ho are nicely reproduced. While the parameters deduced from the experiment for the $K = \frac{11}{2}$ γ-vibrational bands are identical for both nuclei within the uncertainties, the theoretical values show differences arising from the microscopic structure of the γ-vibrational modes and their couplings to the unpaired neutron (^{167}Er) or proton (^{165}Ho). The calculations slightly overestimate the value of Q_1/Q_0 in ^{165}Ho and underestimate Q_2/Q_0 in ^{167}Er. It should be noted that the experimental data could have been influenced by the assumption

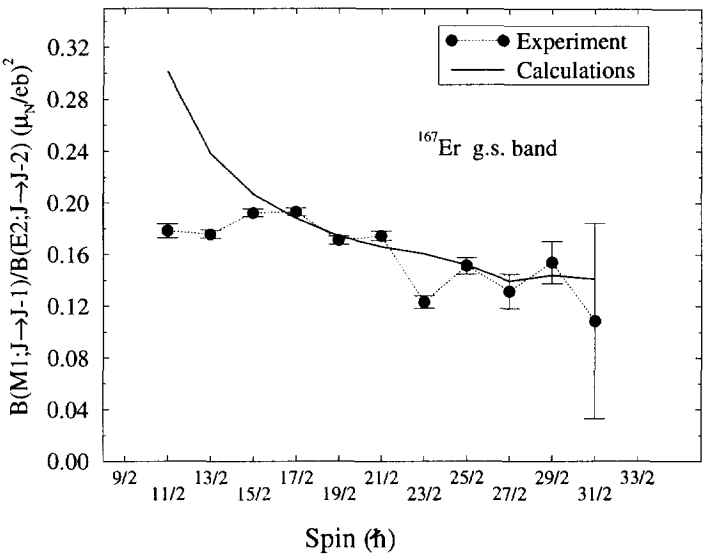

Fig. 11. Transition strength ratio $B(M1)/B(E2)$ for the ground-state band in ^{167}Er. A value of $\delta = 0.28$ was assumed for the mixing ratio [6]. The calculations were performed without the generalized intensity relations.

that the out-of-band transitions did not comprise any M1 component. In spite of this, the agreement between experiment and theory is similar to what was reported for β and γ-vibrational bands in even–even nuclei [9]. This supports the view that the most important aspects of the Coriolis coupling in collective vibrations are well described by the model, for both even–even [16] and odd [17] nuclei.

In the theoretical scheme of generalized γ vibrations, the transition strength ratios $B(M1)/B(E2)$ of the ground-state band of an odd-nucleus are affected by the coupling between the quasiparticle and the γ-vibrational modes [17]. For the ground-state band of ^{167}Er, the transition strength ratios $B(M1)/B(E2)$ have been extracted from the branching ratio λ_{branch} of the in-band decay. Namely, the $B(M1)/B(E2)$ ratios were extracted from the experimental branching ratio with the relation:

$$\frac{B(M1)}{B(E2)} = \frac{0.693}{\lambda_{\text{branch}}(1+\delta^2)} \frac{E_\gamma^5(J \to J-2)}{E_\gamma^3(J \to J-1)} \left(\frac{\mu_n}{\text{eb}}\right)^2, \tag{6}$$

where λ_{branch} is the branching ratio and δ the mixing ratio of the transition. A value of 0.28 was assumed for the mixing ratio which corresponds to the average value reported in Ref. [6]. Calculations have been performed with the Cranked Shell Model + RPA + particle–coupling and following the same approach as in Ref. [17]. The transition probabilities were calculated with the Cranked Shell Model in the high-spin limit (i.e. not with the GIR). Geometrical factors in the transition rates have been added to approximately take into account the angular momentum algebra, following the method in Ref. [22]. In addition to the parameters given in Table 4, a quenching factor of 0.67 (taken from Ref. [8]) was used for the spin g-factors of ^{167}Er. Experimental

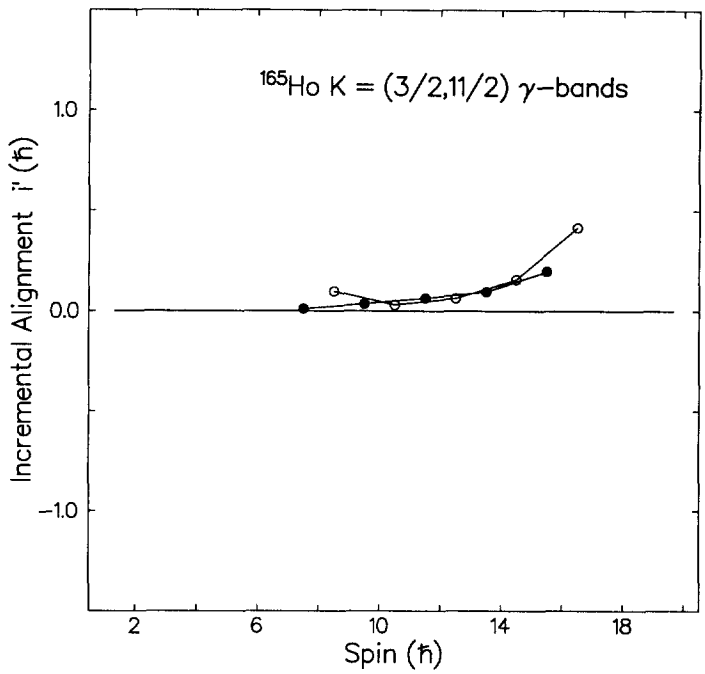

Fig. 12. Incremental alignment between the γ-vibrational bands $K = \frac{11}{2}$ and $K = \frac{3}{2}$ in ^{165}Ho. The $K = \frac{11}{2}$ γ band was used as the reference. Filled (empty) circles correspond to the signature $\alpha = -\frac{1}{2}$ ($\alpha = +\frac{1}{2}$).

and calculated $B(\mathrm{M1})/B(\mathrm{E2})$ are presented in Fig. 11. The excellent agreement for spins higher than $\frac{15}{2}$ shows that the coupling of the quasiparticle with the generalized γ-vibrational modes is essential to reproduce the $B(\mathrm{M1})/B(\mathrm{E2})$ ratios. However, the calculations fail to reproduce the $B(\mathrm{M1})/B(\mathrm{E2})$ ratios at lower spins. The calculated $B(\mathrm{M1})/B(\mathrm{E2})$ ratios increase considerably as the spin decreases. The E2 transition probability decreases more rapidly than the M1 probability; this behaviour is directly related to the exact Clebsch–Gordan coefficients or to the geometrical factors used in the calculations. It should be pointed out that calculations performed with a full treatment of the angular momentum algebra such as the GIR gave similar results. The constancy of the data indicates either that the conventional rotor model is inappropriate or the intrinsic amplitudes (g-factors and/or quadrupole moments) are not constant near the bandhead.Although the microscopic model reproduces the transition ratios at high spins rather well, the low-spin experimental results suggest the necessity of further theoretical and experimental investigations near the bandhead. For example, it would be important to measure accurately the absolute E2 and M1 transition probabilities. A signature dependence in the $B(\mathrm{M1})/B(\mathrm{E2})$ ratios is also observed at higher spins. Similarly to the trend seen in the calculations for signature splitting energies (see Fig. 8), the calculations underestimate the magnitude of this $B(\mathrm{M1})/B(\mathrm{E2})$ staggering.

One of the striking aspects of the data is that the two γ-vibrational bands in ^{165}Ho are

isospectral, i.e., they have very nearly identical γ-ray energies for the in-band transitions originating from states of the same spin. To illustrate the identical character of these γ-vibrational bands, a plot of the incremental alignment [23] between the two bands is shown in Fig. 12. Up to spin $\frac{29}{2}$, the value of the incremental alignment is less than $0.1\hbar$. At that point, the bands appear to enter a backbending region, producing an increase in the incremental alignment. This is the first case where isospectral bands were observed in the same nucleus. The peculiar feature of these identical bands is that they arise through a simple coupling of the collective and single-particle degrees of freedom, rather than through the addition or removal of nucleons. These identical transition energies observed for the $K_>$ and $K_<$ γ bands in ^{165}Ho are not expected from our calculations. In the simplest picture, where the vibration is only a spectator, i.e. does not affect the moment of inertia, the identical transition energies of the γ bands is trivial. However, the quasiparticle–vibration coupling is non-negligible; the typical magnitude of correlation energy is as large as 100 keV when such a coupling is considered. Moreover, the calculated effects of the coupling on the transition energies are always much larger than 1 keV, the experimental accuracy. As the moments of inertia in identical superdeformed bands are unaffected by the polarization effects due to the addition or removal of nucleons, the γ bands in ^{165}Ho present a striking example where the moment of inertia is unaffected by the coupling of the vibration, i.e. independent of the K quantum number.

6. Summary and conclusion

Heavy-ion induced Coulomb excitation experiments performed on ^{165}Ho and ^{167}Er have been analysed in this work. It was found that the nuclei in this mass region were not stopped quickly enough in gold-backed targets to allow the observation of states at spins higher than $\sim\frac{39}{2}$. The study of the decay-out transitions from the γ-vibrational bands to the ground-state band led to a determination of the ratio of the intrinsic quadrupole moments $Q_{\text{out}}/Q_{\text{in}}$, which provided information on the collectivity and the Coriolis mixing for these bands. It was found that the use of the Cranked Shell Model + RPA + particle–vibration coupling within the framework of the unified model reproduced the most important aspects of the Coriolis coupling for the collective γ vibrations in odd-mass nuclei. The $B(\text{M1})/B(\text{E2})$ ratios of the ground-state band are well-described at spin higher than $\frac{15}{2}$ by the model that includes the coupling between quasiparticle and γ-vibrational modes. However, these calculations do not explain the constancy of the $B(\text{M1})/B(\text{E2})$ ratios at low spins. The signature splitting energies in both nuclei and the isospectral properties of the $K = \frac{11}{2}$ and $K = \frac{3}{2}$ γ bands in ^{165}Ho cannot be reproduced by the calculations. Surprisingly, the moment of inertia of these two γ bands is found to be independent of the K quantum number.

Acknowledgements

This work was partially supported by the Natural Sciences and Engineering Research Council of Canada (NSERC), AECL and by the Grant-in-Aid for Scientific Research from the Japan Ministry of Education, Science and Culture (No. 08640383 and 08740209). One of the authors (G.G.) acknowledges receipt of a scholarship from Fonds pour la Formation de Chercheurs et l'Aide à la Recherche du Gouvernement du Québec (FCAR).

References

[1] Th. Byrski, F.A. Beck, D. Curien, C. Schuck, P. Fallon, A. Alderson, I. Ali, M.A. Bentley, A.M. Bruce, P.D. Forsyth, D. Howe, J.W. Roberts, J.F. Sharpey-Schafer, G. Smith and P.J. Twin, Phys. Rev. Lett. 64 (1990) 1650.
[2] C. Baktash, B. Haas and W. Nazarewicz, Ann. Rev. Nucl. Part. Sci. 45 (1995) 485.
[3] R.M. Diamond, B. Elbek and F.S. Stephens, Nucl. Phys. 43 (1963) 560;
G.G. Seaman, E.M. Bernstein and J.M. Palms, Phys. Rev. 161 (1967) 1223.
[4] M.W. Simon, D. Cline, M. Devlin, R. Ibbotson and C.Y. Wu, Proc. Conf. on Physics from Large Gamma-ray Det. Arrays, Berkeley CA, Vol. 1 (1994) p. 114.
[5] A. Tveter and B. Herskind, Nucl. Phys. A 134 (1969) 599.
[6] M. Ohshima, E. Minehara, M. Ishii, T. Inamura and A. Hashizume, Nucl. Phys. A 436 (1985) 518.
[7] E.R. Marshalek, Phys. Rev. C 11 (1975) 1426; Nucl. Phys. A 266 (1976) 317.
[8] A. Bohr and B.R. Mottelson, Nuclear Structure, Vol. 2 (Benjamin, New York, 1975) Chap. 4.
[9] Y.R. Shimizu and T. Nakatsukasa, Nucl. Phys. A 611 (1997) 22.
[10] D. Cline, Ann. Rev. Nucl. Part. Sci. 36 (1986) 683.
[11] H.R. Andrews, P. Taras, J.C. Waddington and D. Ward, Proposal for a National Facility-The 8π Spectrometer, AECL-8329 (1984).
[12] D.C. Radford, Nucl. Instr. and Meth. A 361 (1995) 297.
[13] V.S. Shirley, Nucl. Data Sheet 58 (1989) 871.
[14] D. Ward, H.R. Andrews, G.C. Ball, A. Galindo-Uribarri, V.P. Janzen, T. Nakatsukasa, D.C. Radford, T.E. Drake, J. DeGraaf, S. Pilotte and Y.R. Shimizu, Nucl. Phys. A 600 (1996) 88.
[15] J.L. Egido, H.J. Mang and P. Ring, Nucl. Phys. A 339 (1980) 390.
[16] Y.R. Shimizu and K. Matsuyanagi, Prog. Theor. Phys. 79 (1983) 144; 72 (1984) 799.
[17] M. Matsuzaki, Y.R. Shimizu and K. Matsuyanagi, Prog. Theor. Phys. 79 (1988) 836.
[18] Y.R. Shimizu and M. Matsuzaki, Nucl. Phys. A 588 (1995) 559.
[19] S.A. Hjorth, H. Ryde, K.A. Hagemann, G. Løvhøiden and J.C. Waddington, Nucl. Phys. A 144 (1970) 513.
[20] D.R. Bes and Cho Yi-Chung, Nucl. Phys. 86 (1966) 581.
[21] V.M. Mikhailov, Izv. Akad. Nauk. USSR, Ser. Fiz. 30 (1966) 1334;
B.R. Mottelson, Proc. Int. Conf. on Nucl. Str., Tokyo (1967) p. 87.
[22] M. Oshima, M. Matsuzaki, S. Ichikawa, H. Iimura, H. Kusakari, T. Inamura, A. Hashizume and M. Sugawara, Phys. Rev. C 40 (1989) 2084.
[23] F.S. Stephens, M.A. Delaplanque, J.E. Draper, R.M. Diamond, A.O. Macchiavelli, C.W. Beausang, W. Korten, W.H. Kelly, F. Azaiez, J.A. Becker, E.A. Henry, S.W. Yates, M.J. Brinkman, A. Kuhnert and J.A. Cizewski, Phys. Rev. Lett. 65 (1990) 301.